Geophysical Research Letters

RESEARCH LETTER
10.1029/2019GL084079

An Interdecadal Shift of the Extratropical Teleconnection From the Tropical Pacific During Boreal Summer

Christopher H. O'Reilly[1], **Tim Woollings**[1], **Laure Zanna**[1], **and Antje Weisheimer**[1]

[1]Atmospheric, Oceanic and Planetary Physics, Oxford, UK

Abstract The extratropical teleconnection from the tropical Pacific in boreal summer exhibits a significant shift over the past 70 years. Cyclonic circulation anomalies over the North Atlantic and Eurasia associated with El Niño in the later period (1978–2014) are absent in the earlier period (1948–1977). An initialized atmospheric model ensemble, performed with prescribed sea surface temperature (SST) boundary conditions, replicates some key features of the shift in the teleconnection, providing clear evidence that this shift is not simply due to internal atmospheric variability or random sampling. Additional ensemble simulations, one with detrended tropical SSTs and another with constant external forcing are analyzed. In the model, the teleconnection shift is associated with climatological atmospheric circulation changes, which are substantially reduced in the simulation with detrended tropical SSTs. These results demonstrate that the climatological atmospheric circulation and associated teleconnection changes are largely forced by tropical SST trends.

Key Points:
- The extratropical summer teleconnection from the tropical Pacific strengthens over the North Atlantic and Eurasia during the last 70 years
- The teleconnection shift is reproduced in an atmospheric model, providing clear evidence that it is not due to internal atmospheric variability
- Further ensemble model simulations show that tropical SST trends have played an important role in shifting the ENSO teleconnection pattern

Supporting Information:
- Supporting Information S1

Correspondence to:
C. H. O'Reilly,
christopher.oreilly@physics.ox.ac.uk

Citation:
O'Reilly, C. H., Woollings, T., Zanna, L., & Weisheimer, A. (2019). An interdecadal shift of the extratropical teleconnection from the tropical Pacific during boreal summer. *Geophysical Research Letters*, *46*, 13,379–13,388. https://doi.org/10.1029/2019GL084079

Received 12 JUN 2019
Accepted 3 SEP 2019
Accepted article online 12 SEP 2019
Published online 26 NOV 2019

1. Introduction

El Niño–Southern Oscillation (ENSO) is the dominant mode of interannual climate variability in the tropics. The anomalous distribution of sea surface temperatures (SSTs) in the tropical Pacific and associated precipitation anomalies not only affect climate in the tropical regions but also influence remote regions in the extratropics, often referred to as *teleconnections*, by exciting Rossby wave propagation (e.g., Hoskins and Karoly; 1981; Sardeshmukh and Hoskins; 1988; Trenberth et al. 1998). In summer the tropical Pacific SST anomalies are weaker than in the winter season, and the teleconnections to the extratropics are also typically weaker. Nonetheless, numerous studies have demonstrated that tropical Pacific SST anomalies influence the northern extratropics during summer, with significant influences on climate across continental regions of North America and Eurasia (e.g., O'Reilly et al., 2018; Ropelewski & Halpert, 1987; Shaman, 2014b, 2014a; Shaman & Tziperman, 2007; Wulff et al., 2017). The teleconnection to the extratropics during boreal summer is largely consistent with barotropic Rossby wave propagation driven by precipitation anomalies in the tropical Pacific (O'Reilly et al., 2018; Shaman, 2014b; Shaman & Tziperman, 2011).

During the winter season, the extratropical ENSO teleconnection in the North Pacific has exhibited substantial multidecadal variability, which appears to be due to variability in the amplitudes of ENSO events themselves (e.g., Diaz et al., 2001; Minobe & Mantua, 1999; O'Reilly, 2018; O'Reilly et al., 2017). There is also some evidence that the summer teleconnection from the tropical Pacific to the extratropics exhibits variability on multidecadal time scales. In a recent paper, O'Reilly et al. (2018) found that the observed summer teleconnection from the tropical Pacific to the North Atlantic sector is seemingly absent before 1978 or so. The cause of this changing summer teleconnection, however, is not clear. It is possible that the variability in the summer teleconnection is due to random internal atmospheric variability. An example of such internal atmospheric variability in the literature is the decadal variability in the relationship between ENSO and Indian Monsoon precipitation. Model simulations with observed (prescribed) SSTs do not seem able to account for the variable relationship between ENSO and Indian Monsoon precipitation, and it has been argued that the variability is indistinguishable from random sampling (e.g., Cash et al., 2017; DelSole & Shukla, 2012; Gershunov et al., 2001; Yun & Timmermann, 2018). However, if model simulations are able to replicate the observed changes in the summer teleconnection this would provide evidence that the changes in the teleconnection represent real changes in the climate system, rather than sampling of random internal atmospheric variability.

In this study, we investigate the shifting summer teleconnection from the tropical Pacific to the extratropics from 1948 onward, using reanalysis data sets and a series of atmospheric general circulation model (AGCM) simulations. The extratropical teleconnection shift observed around the late 1970s is well captured in the AGCM using observed SSTs with varying greenhouse gas concentrations and other external forcings. Further AGCM experiments reveal that the forced and/or natural tropical SST trends likely contribute to the changes in the observed teleconnection.

2. Data and Methods

2.1. Observational and Reanalysis Data Sets

In this study we analyze data from the NCEP-NCAR reanalysis (Kalnay et al., 1996) over the period 1948–2014. In addition, we analyze data from the Twentieth Century Reanalysis (20CR; Compo et al., 2011) and European Centre for Medium-Range Weather Forecasts (ECMWF) reanalysis (ERA). Since none of the individual EMWF reanalysis products span the whole 1948–2014 period, the ERA data set defined here uses ERA-Interim reanalysis between 1979 and 2014 (Dee et al., 2011), ERA-40 between 1958 and 1978 (Uppala et al., 2005), and ERA-20C between 1948 and 1957 (Poli et al., 2016). This combined ERA data set was also used to initialize the atmospheric model simulations (see next subsection). In general, the results are qualitatively similar across the different reanalysis data sets and lead to consistent conclusions; however, where the results are not consistent across the reanalysis products, this is explicitly discussed. In addition to the reanalysis data sets, we analyze the gridded surface air temperature data from the CRU-TS v4.01 data set (Harris et al., 2014) and SST data from the HadISST data set (Rayner et al., 2003). We analyze teleconnections associated with the "Niño 3.4 Index," which is the area-averaged SST anomaly between 5°S to 5°N and 170–120°W (e.g., Trenberth, 1997).

Statistical significance was calculated using Monte Carlo resampling techniques—see Text S1 in the supporting information for a detailed description.

2.2. Atmospheric Model Simulations

Atmospheric model simulations were performed using initialized integrations of ECMWF's Integrated Forecasting System (IFS), cycle 41r1. The simulations were performed a horizontal resolution of T255 (≈80 km), with 60 vertical levels up to 0.01 hPa at the highest level. The experiments employed prescribed SST and sea ice boundary conditions from the HadISST data set. These simulations include prescribed variation of external forcings, including varying greenhouse gas concentrations, volcanic aerosol loading in the stratosphere, and variable solar forcing. We initialized seasonal integrations each year between 1948 and 2014, on 1 May in each year. The model initial conditions were taken from the combined ERA reanalysis data set (i.e., ERA-20C, ERA-40, and ERA-Interim) as outlined above. This data set was selected as the most comprehensive ECMWF reanalysis product available for each year of the simulations. For each year in each simulation, 10 ensemble members were integrated through the end of August, to allow us to analyze the June-July-August boreal summer season. The experiments were performed using explicit stochastic physics, which represents unresolved subgrid-scale atmospheric processes, and this creates spread across ensemble members (e.g., Weisheimer et al., 2017).

The "CONTROL" experiment used the setup outlined above. A second experiment was performed with detrended SSTs in the tropics, hereafter referred to as "TROPdetrend." The SSTs in TROPdetrend are the same observed SSTs as in the CONTROL ensemble but a seasonally varying trend (31-day moving average) calculated over the period 1948–2014 was removed at each gridpoint between 20°S and 20°N. The SSTs in TROPdetrend, therefore, maintain all high-frequency variability in the tropics. The detrending has a linear tapering between 20–30°S and 20–30°N, such that SSTs poleward of 30°N and 30°S are identical to the CONTROL experiment. A third experiment was performed as in CONTROL but with fixed external forcings, hereafter referred to as "EXTconst." The EXTconst experiment has greenhouse gas concentrations fixed at 1,990 levels, no stratospheric volcanic aerosol loading and no solar variability. It should be noted that the large-scale SST warming trend in the tropics is mostly forced by increasing greenhouse gas concentrations, mainly CO_2, so the EXTconst ensemble excludes the direct CO_2 response (e.g., Bony et al., 2013).

3. Results

O'Reilly et al. (2018) showed that the boreal summer teleconnection from the tropical Pacific to the North Atlantic sector—in terms of tropospheric circulation anomalies—differs before and after the 1970s in observations. Here we analyze this apparent shift in the summer teleconnection over the Northern Hemisphere between the early period, 1948–1977, and the late period, 1978–2014. Correlation maps between the Niño 3.4 index and the 300 hPa geopotential height, Z_{300}, from the NCEP-NCAR reanalysis are shown in Figures 1a, 1c, and 1e for the early, late period, and the difference (defined as late minus early). Over the late period, there are substantial cyclonic circulation anomalies (i.e., negative correlations) over the North Atlantic, Eastern Europe, and the western North Pacific, which are almost absent in the early period, suggesting a shift in the teleconnection between these two periods. The shift in the summer teleconnection is also evident in the surface temperature, shown in Figure 1i, with substantial correlation differences seen across much of the Eurasian continent. Therefore, despite considerable sampling uncertainty, there seems to be consistent observational evidence indicating that there has been a shift in the boreal summer teleconnection from the tropical Pacific over the past 70 years.

We now examine whether the shift in the teleconnection is forced, that is, through changes in SSTs or external forcing, or is due to internal atmospheric variability, using the 10-member CONTROL ensemble. Correlation maps between the Niño 3.4 index and the ensemble mean Z_{300} in the CONTROL ensemble for the early period, late period and the difference are shown in Figures 1b, 1d, and 1f, alongside the equivalent maps from reanalysis. The teleconnection in the CONTROL ensemble captures many features in the reanalysis, in both the early and late periods. For example, in the late period the centers of negative correlation over the western North Pacific, the midlatitude North Atlantic, and over Eurasia are clear in the CONTROL ensemble, albeit with a slight longitudinal offset (Figure 1b). In the early period, the characteristics of the extratropical teleconnection change substantially; the centers of negative correlation in the late period are weakened and even replaced by positive correlations over Eurasia. This interdecadal shift in the extratropical teleconnection in the CONTROL ensemble is clear in the difference map (Figure 1f), particularly over the midlatitude North Atlantic and the Eurasian continent. The difference in the correlations of surface temperatures with Niño 3.4 in the CONTROL ensemble are also similar to that seen in observations, most notably over the Eurasian continent, consistent with the difference in the large-scale circulation response to tropical Pacific SST anomalies (Figure 1h). Since significant aspects of the shift in the extratropical teleconnection during summer are captured in the CONTROL ensemble, we can conclude that the interdecadal shift in the teleconnection is not simply due to internal atmospheric variability.

To further investigate the nature of teleconnection change over the analysis period, we examine the evolution of the correlation of the Z_{300} anomalies with the Niño 3.4 index over moving 25-year windows, plotted in Figure 2 for North Atlantic and Eurasian regions (outlined in Figure 1). In the reanalysis data sets, there are no significant correlations between Z_{300} and the Niño 3.4 index over the earlier periods but, moving to more recent periods, the correlations strengthen as data from the late-1970s and later are included in the window, for both the North Atlantic and Eurasian indices (Figures 2a and 2b). Comparative plots for the CONTROL ensemble are shown in Figures 2c and 2d. The correlation between Z_{300} in the North Atlantic and Eurasian regions and the Niño 3.4 index shows a similarly weak (or even positive) correlation as the reanalysis in the early period in both regions, becoming significantly stronger in the later periods.

Also shown in Figures 2c and 2d is the correlation calculated over all ensemble members in each 25-year window. The observed teleconnection can in one sense be considered a "single realization," so the strength of the teleconnection across the individual members is more suitable to compare with the reanalysis. The shift in the teleconnection to the North Atlantic and Eurasian regions across all ensemble members is qualitatively very similar to the ensemble mean—weak (or even positive) in the early periods becoming negative in the recent periods. However, the magnitude of the correlation is substantially lower than in the reanalysis when calculated across all ensemble members. This indicates that while the model captures well some of the distinct observed changes in the extratropical teleconnection, the model response has weaker teleconnections to the extratropics than in the observational data sets.

We now investigate what has caused the teleconnection to change over the past 70 years. A notable feature of the changing teleconnection, in both the reanalysis and CONTROL ensemble (Figure 2), is the reasonably steady shift toward negative correlation between the Niño 3.4 index and the North Atlantic and Eurasian

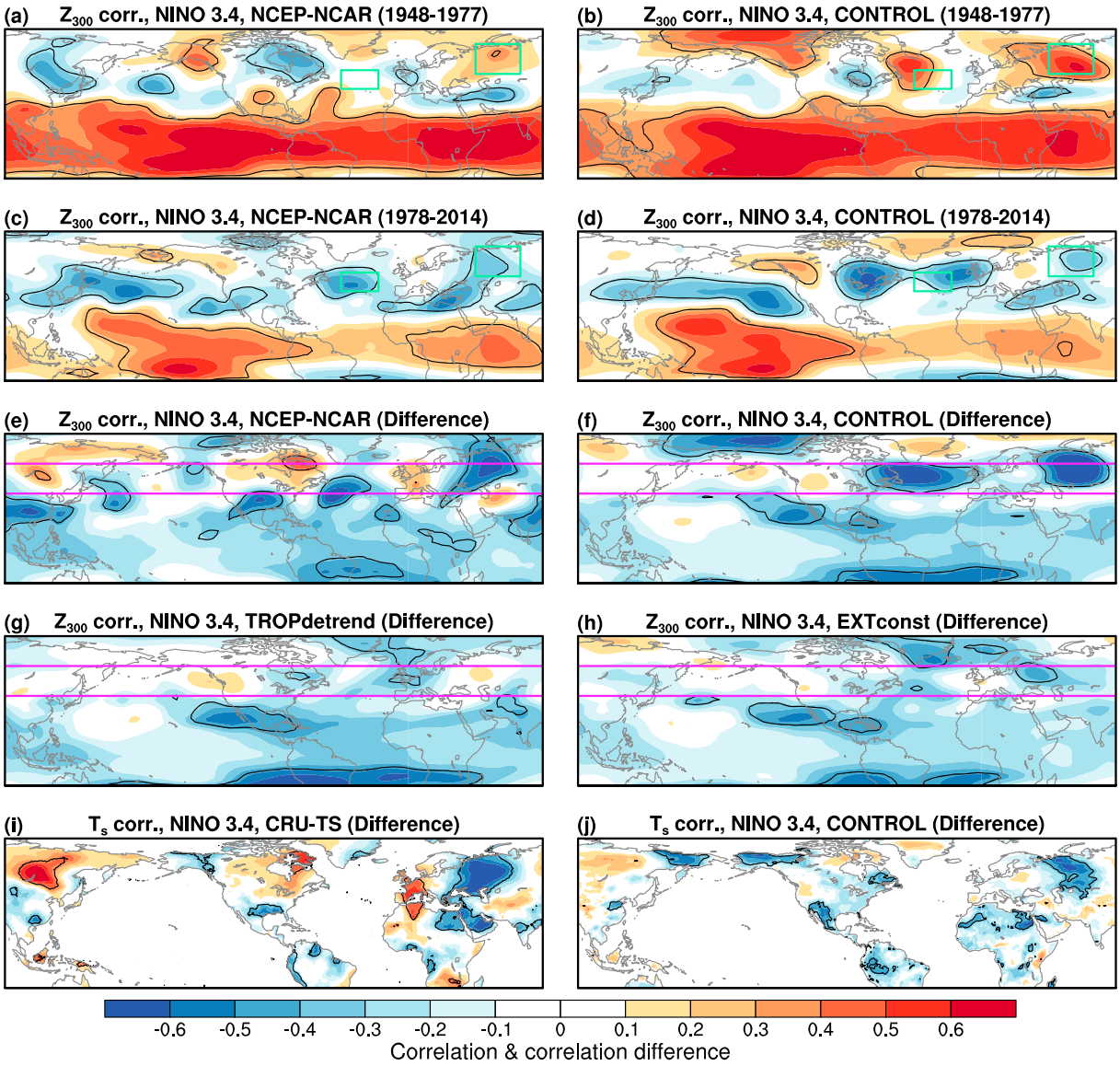

Figure 1. Correlation between the summer (June-July-August) Z(300 hPa) and the Niño-3.4 index during (a) the early period, 1948–1977, and (c) the late period, 1978–2014 in the NCEP-NCAR reanalysis. (b and d) As in (a and c) but for the ensemble mean of the CONTROL ensemble. The difference between the Z(300 hPa) correlation maps, defined as late period minus the early period, is shown for (e) the NCEP-NCAR reanalysis and (f) the CONTROL ensemble. The Z(300 hPa) correlation difference is also shown for (g) the TROPdetrend ensemble and (h) the EXTconst ensemble. The correlation difference is also shown for surface air temperature in (i) the CRU-TS data set and (j) the CONTROL ensemble. Black contours indicate where the correlation and correlation difference are found to be significant at the 5% level (using Monte Carlo resampling, see Text S1 in the supporting information). The green boxes in (a)–(d) indicate the region used to compute the North Atlantic Z_{300} index plotted in Figure 2. The midlatitude band, shown in magenta in (e)–(h), indicates the region used to plot the midlatitude Z_{300} correlation difference in Figure 4.

indices. Over the last 70 years there have been significant warming trends due to increases in greenhouse gas concentrations, and a prominent feature is the tropical SST trend outside of the eastern equatorial Pacific (Deser et al., 2010). The tropical SST trends are clear in the epoch difference in SST between the early (i.e., 1948–1977) and late (i.e., 1978–2014) periods of the present analysis, shown in Figure 3a. To examine the importance of these tropical SST changes on the extratropical teleconnection we have performed an ensemble simulation in which the tropical SSTs have been detrended—the TROPdetrend ensemble. To assess the likely direct impact of atmospheric greenhouse gas concentrations, we performed an additional ensemble simulation that was the same as the CONTROL ensemble but with greenhouse gas concentrations and other external forcings fixed—the EXTconst ensemble. It is worth noting at this

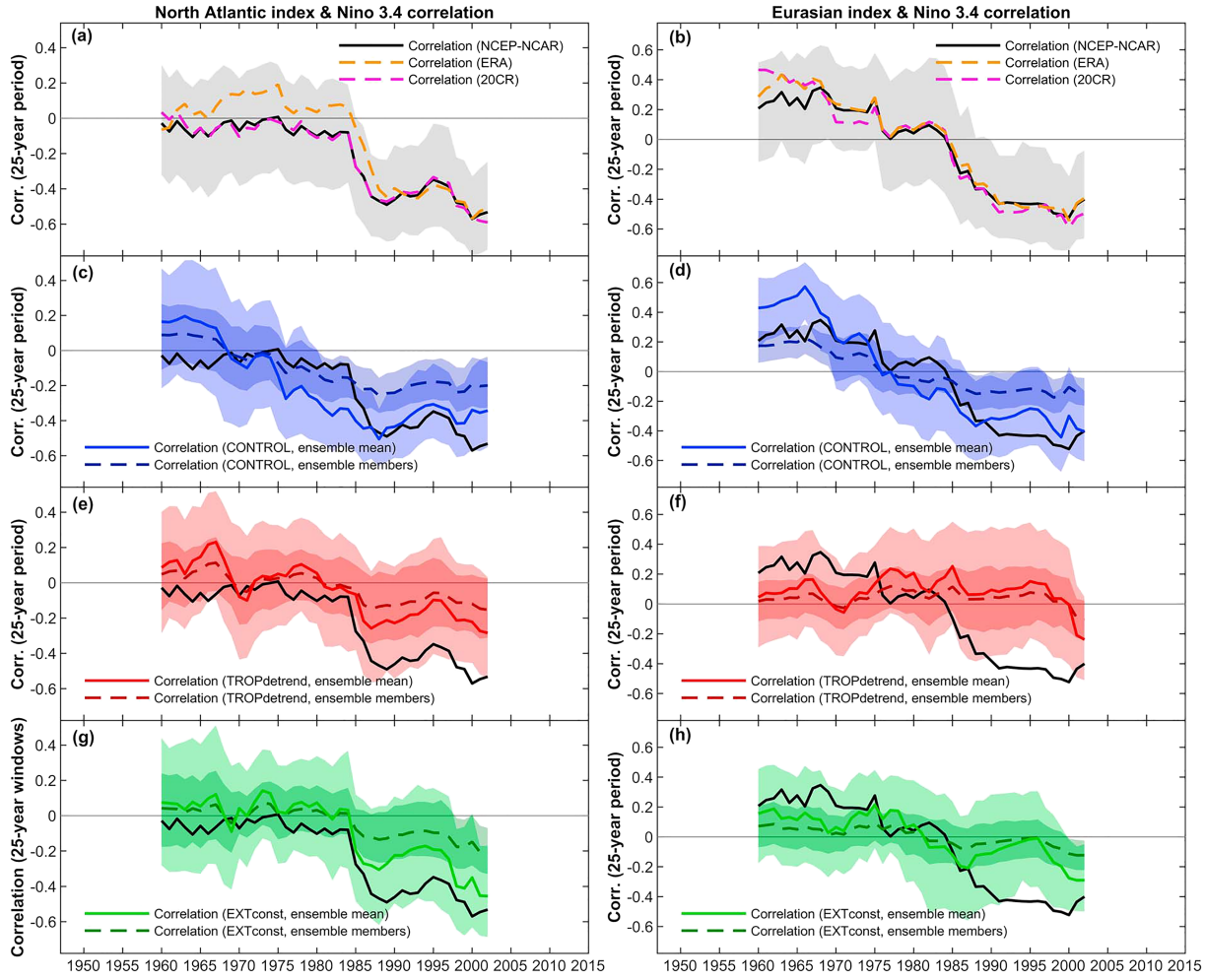

Figure 2. Correlation between the summer (June-July-August) North Atlantic circulation index (green box in Figure 1a) and the Niño 3.4 Index for (a) the NCEP-NCAR, ERA, and 20CR data sets; (c) CONTROL ensemble; (e) TROPdetrend ensemble; (g) EXTconst ensemble. The shading in each plot shows the 5–95% confidence interval of the correlation (though only for NCEP-NCAR in panel a). In panels (c), (e), and (g) the solid lines indicate correlations between the ensemble mean Z_{300} anomaly and Niño-3.4, whereas dashed lines indicate correlations across all ensemble members and Niño-3.4. The correlation calculated from NCEP-NCAR is replotted in (c), (e), and (g) for reference. (b, d, f, and h) As in (a, c, e, and g) but for the correlation between the Eurasian index and Niño 3.4.

point that the variance and spatial distribution of the summer SST anomalies associated with the Niño 3.4 Index in the tropical Pacific are not substantially different between the two periods in observations, though there is perhaps a slight eastward shift (Figures 3b–3d). The similarity of the tropical Pacific SST anomalies across the two periods suggests that changes in the nature of SST variability may not be responsible for the shift in the teleconnection patterns.

The correlations between the Niño 3.4 index and the North Atlantic and Eurasian indices in the TROPdetrend and EXTconst ensembles are shown in Figure 2. In the TROPdetrend ensemble the shifting teleconnection is essentially absent in both the North Atlantic and Eurasian regions (Figures 2e and 2f). While there is a small hint of a shift toward a negative correlation in the North Atlantic in later periods, the shift is very weak compared to the CONTROL ensemble and is not statistically significant. Over the Eurasian region there is no shift in the teleconnection whatsoever in the TROPdetrend ensemble. In the EXTconst ensemble, the shifting teleconnection is more similar to the CONTROL ensemble, compared to the TROPdetrend ensemble, but the shifts are substantially weaker (Figures 2g and 2h). Only in the later periods does the teleconnection exhibit significant correlation with the North Atlantic and Eurasian indices in the EXTconst ensemble.

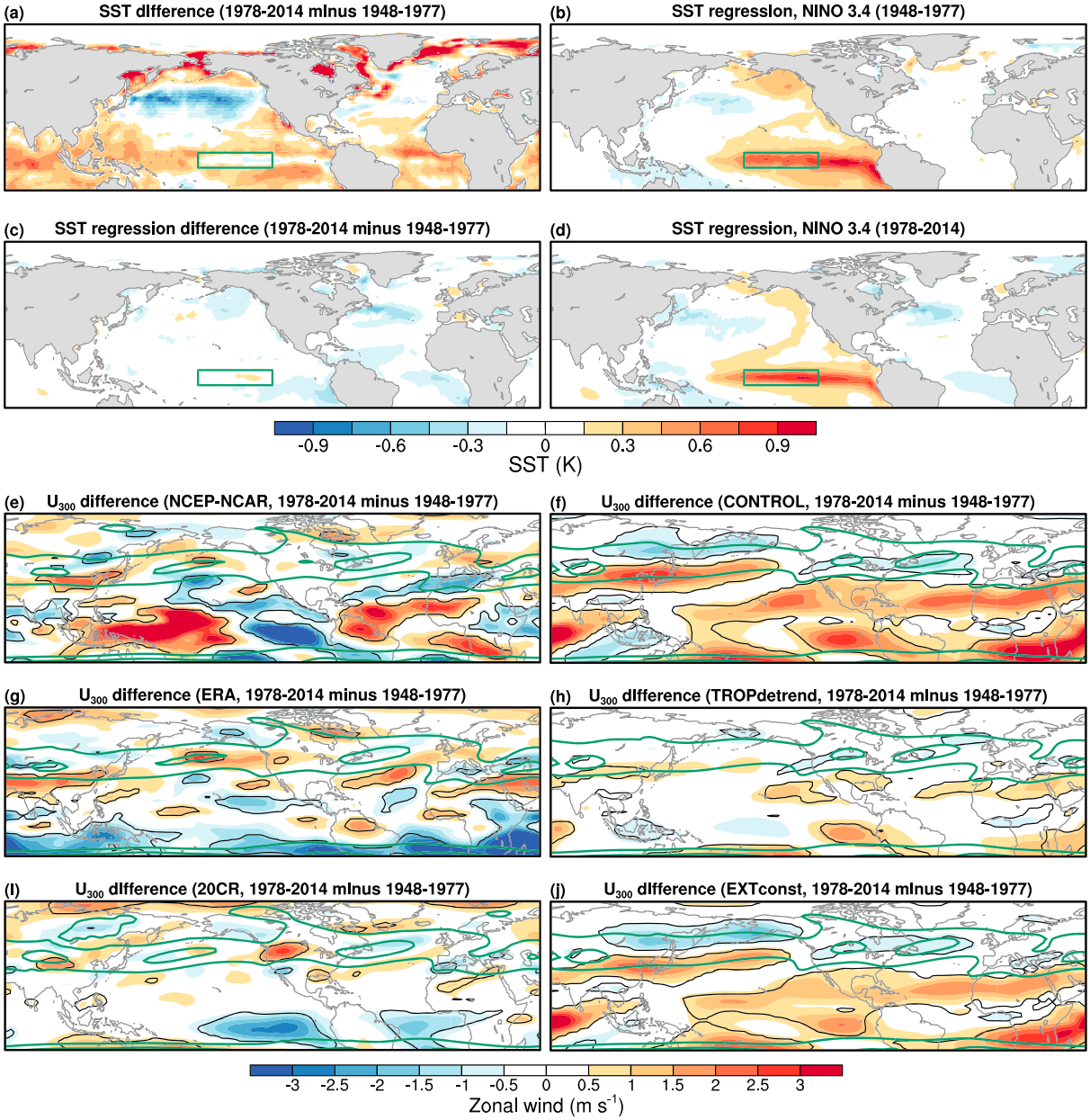

Figure 3. (a) Climatological (June-July-August) sea surface temperature (SST) epoch difference, 1978-2014 minus 1948–1977. SST regressed on the normalized Niño-3.4 index for (b) 1948–1977 and (d) 1978–2014. (c) The difference in the SST regression, 1978–2014 minus 1948–1977. The climatological upper tropospheric zonal wind epoch differences, 1978–2014 minus 1948–1977, are also plotted for (e) NCEP-NCAR reanalysis; (g) ERA reanalysis; (i) 20CR reanalysis; (f) CONTROL ensemble; (h) TROPdetrend ensemble; and (j) EXTconst ensemble. In panels (a)–(d) all shaded regions are significant at the 5% level. In panels (e)–(j) anomalies that are significant at the 5% level are shown in black contours. The green contours show the climatological zonal wind over the whole analysis period (i.e., 1948–2014), contoured at 10 and 20 m/s. Green boxes in panels (a)–(d) shows the Niño-3.4 region.

We now compare the difference in the extratropical teleconnection between the early and late periods across the experiments. To do this we calculated the difference in the correlation between the Niño 3.4 index and Z_{300} over the midlatitudes (shown for each of the simulations in Figures 1f–1h), which are plotted in Figure 4. The significant differences in the extratropical teleconnection in the reanalysis and CONTROL ensemble around 60°E and 330°E are completely absent in the TROPdetrend ensemble (Figure 4c). The difference in the extratropical teleconnection in the EXTconst ensemble is qualitatively similar to the CONTROL ensemble but weaker and the differences around 60°E and 330°E are not clearly significant compared to sampling variability. The results from the TROPdetrend and EXTconst ensembles

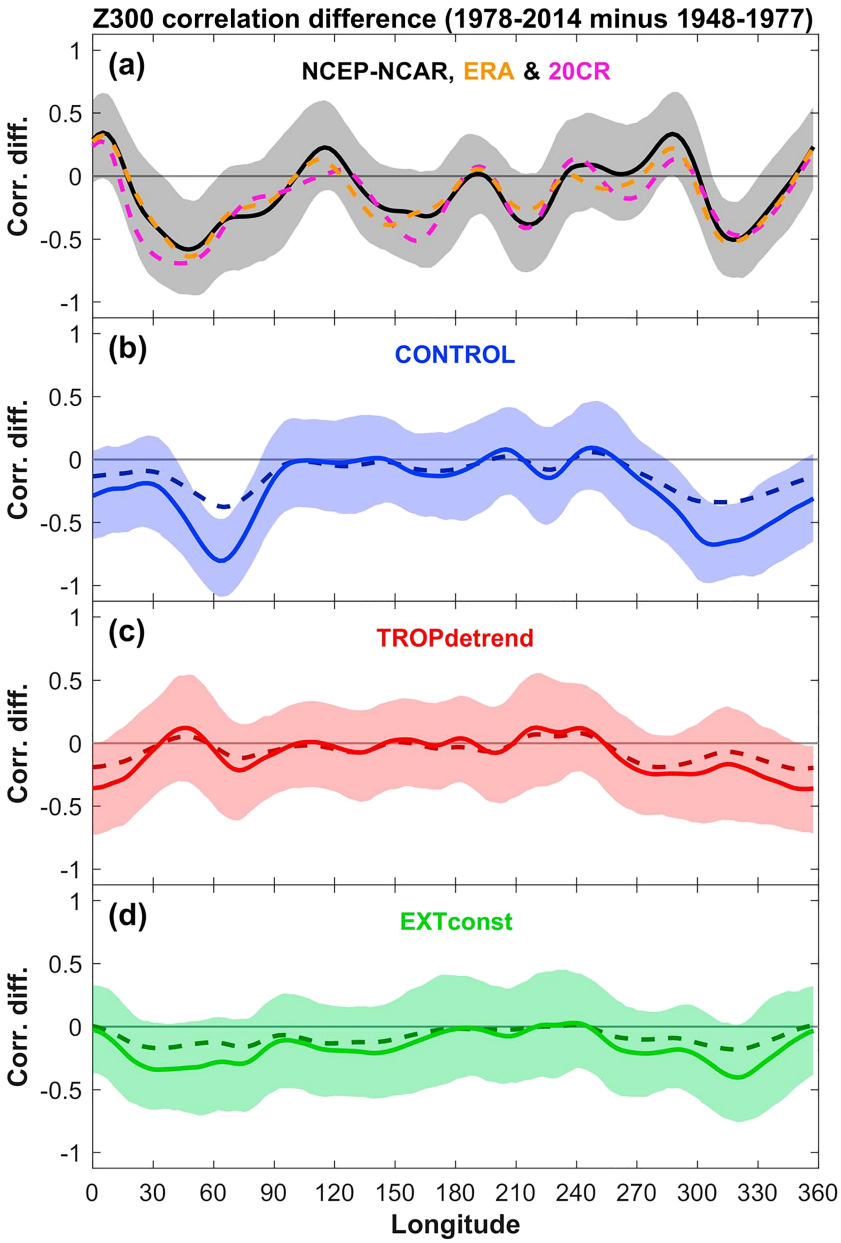

Figure 4. Midlatitude Z_{300} versus Niño 3.4 correlation difference (i.e., 1978–2014 minus 1948–1977) for the following: the NCEP-NCAR, ERA, and 20CR data sets; (b) CONTROL ensemble; (c) TROPdetrend ensemble; (d) EXTconst ensemble. In (b)–(d) the solid colored lines indicate the correlation between the ensemble mean Z_{300} anomaly and Niño-3.4, whereas the dashed line indicates the correlation across all ensemble members and the Niño-3.4 index. The shading shows the 5–95% confidence interval based on a bootstrap-with-replacement resampling for NCEP-NCAR in panel (a) and for the ensemble mean correlation difference in panels (b)–(d).

demonstrate that tropical SST trends are an important factor in generating the shift in the extratropical teleconnection in the CONTROL ensemble and reanalysis. However, the tropical SST trends are included in the EXTconst experiment which is not able to capture the strength of the teleconnection shift seen in the CONTROL ensemble, indicating that the external forcing plays a secondary but necessary direct role in generating the teleconnection shift.

To further examine why the teleconnection has shifted over the past 70 years it is useful to analyze the circulation changes in the upper troposphere. The climatological upper-tropospheric circulation has been shown to have an important influence on the stationary Rossby wave response to tropical forcing

anomalies in simple and more comprehensive models (e.g., Branstator, 1983; Dawson et al., 2011). Maps of the epoch differences (i.e., late period minus early period) for the reanalysis and the model simulations are shown in Figures 3e–3j. All the reanalysis data sets suggest there is some difference in the climatological background circulation between the two periods but there is large uncertainty between the data sets. This uncertainty is likely due to the paucity of upper-level observations prior to the satellite era (i.e., 1979 onward) and the different models used to produce the reanalysis products where there are poor observational constraints.

The epoch difference maps from the ensemble model simulations, however, are less uncertain and might offer some insight. In the CONTROL ensemble there are substantial upper-level jet differences between the early and late periods across much of the midlatitudes and particularly in the region of the western North Pacific jet. In the TROPdetrend ensemble, the upper-level jet differences are largely absent, particularly compared to the CONTROL ensemble. In the EXTconst ensemble, the upper-level jet differences are similar to the CONTROL ensemble in pattern but with a weaker amplitude. To quantify the relative contributions of the Tropical SST trends and external forcings, we performed a simple linear regression analysis targeting the CONTROL epoch difference fields with the TROPdetrend and EXTconst epoch difference fields (i.e., Figures 4f, 4h, and 4j). The best fit between 20°S and 80°N was found to be $\Delta U_{\mathrm{CONTROL}}=1.21\times\Delta U_{\mathrm{EXTconst}}$ for the EXTconst ensemble (spatial correlation of $r=0.96$) and $\Delta U_{\mathrm{CONTROL}}=1.97\times\Delta U_{\mathrm{TROPdetrend}}$ for the TROPdetrend ensemble (spatial correlation of $r=0.83$). Therefore, the epoch difference in the upper-level jet is almost 20% smaller in the EXTconst ensemble than in the CONTROL ensemble but the pattern of change is very similar. The epoch difference in the TROPdetrend ensemble is about 50% smaller than in the CONTROL ensemble and the pattern is not as similar as in the EXTconst ensemble. This analysis indicates that the distinct differences in the upper-level jet climatology in the CONTROL ensemble are primarily driven by the tropical SST trend, while the direct influence of varying external forcings (e.g., greenhouse gases) plays a secondary role.

The epoch difference maps of precipitation (Figure S1) show that the warm pool precipitation increases in the CONTROL ensemble—broadly similar to that seen in Global Precipitation Climatology Project observational data set—and this seems to be driven primarily by the warming in the western Tropical Pacific (Figure 3a). These precipitation changes are consistent with a strengthening of the Walker circulation over the last 70 years, as shown in other studies (e.g., L'Heureux et al., 2013). The changes in climatological precipitation in the tropics are much reduced in TROPdetrend, suggesting that these precipitation changes are responsible for changing the climatological background circulation.

4. Concluding Remarks

In this study we have investigated an interdecadal shift in the boreal summer extratropical teleconnection from the tropical Pacific over the last 70 years. In reanalysis data sets there are significant differences between the teleconnection in the periods before and after the late 1970s. The cyclonic circulation anomalies over the North Atlantic and Eurasia associated with El Niño in the late period are absent (or even anticyclonic) in the earlier period. The CONTROL ensemble, performed with prescribed SST boundary conditions is able to replicate some key features of the shift in the teleconnection, which provides strong evidence that this shift is not simply due to internal atmospheric variability or random sampling. However, despite the ensemble mean CONTROL capturing the observed shift, the teleconnection to the extratropics in the individual ensemble members is substantially weaker than that in observations. Additional ensemble simulations, one with detrended tropical SSTs (TROPdetrend) and another with constant external forcing (EXTconst), suggest that the tropical SST trends have played an important role in shifting the extratropical teleconnection pattern over the last 70 years.

The shift in the teleconnection in the model is associated with large-scale changes to the climatological background circulation. These changes are greatly reduced in the TROPdetrend experiment, demonstrating that the changes in climatological atmospheric circulation are largely forced by tropical SST trends. Furthermore, this suggests that the change in climatological atmospheric circulation is responsible for the change in the teleconnection. We tested the impact of the changes of the climatological atmospheric circulation between the early and late periods using a barotropic model with idealized forcing in the tropical Pacific (following; O'Reilly et al., 2018; see Text S2 and Figure S2). The barotropic model does not reproduce the locations and

magnitude of the teleconnection differences particularly well. Nonetheless, the barotropic model experiments reveal that the change in background state can have a substantial impact along the extratropical waveguide in the CONTROL ensemble compared with the TROPdetrend ensemble (Figure S2). However, the response cannot be wholly explained by changes in stationary Rossby waves—at least in this idealized model setup. It could be that the changes in the observed teleconnection reflect changes in subseasonal anomalies that are mediated by the propagation of stationary Rossby wave anomalies from the tropical Pacific. For example, over the Eurasian region, seasonal mean anomalies are linked to the presence of blocking highs, which have occurred more frequently during La Niña years over the past few decades (e.g., Drouard & Woollings, 2018; Schneidereit et al., 2012).

The warming tropical SST trends are predominantly forced by increased greenhouse gas concentrations. Therefore, the shift in the boreal summer teleconnection from the tropical Pacific likely reflects a forced response of interannual variability to climate change. This is an important result because it demonstrates that future changes in the climatological SST distributions in the tropics can influence the patterns of summertime interannual variability in the extratropics associated with ENSO. However, we have demonstrated that the boreal summer teleconnection to the extratropics is sensitive to relatively subtle changes to the climatological atmospheric circulation. This presents a challenge for coupled climate models, which generally have substantial jet biases in the extratropics. Understanding how these biases influence the ENSO teleconnection in these coupled models—and ultimately reducing the biases—is an important factor in simulating how the boreal summer teleconnection will behave over the coming decades.

Acknowledgments
This work is part of the NERC SummerTIME Project (NE/M005887/1) and the EUCP project (EU Horizon 2020, Grant Agreement 776613). The simulations were performed using resources from an ECMWF Special Project (project code: "SPGBOREI"). Monthly gridded data from the simulations described in this article are available on request from the corresponding author.

References

Bony, S., Bellon, G., Klocke, D., Sherwood, S., Fermepin, S., & Denvil, S. (2013). Robust direct effect of carbon dioxide on tropical circulation and regional precipitation. *Nature Geoscience*, *6*(6), 447.

Branstator, G. (1983). Horizontal energy propagation in a barotropic atmosphere with meridional and zonal structure. *Journal of the Atmospheric Sciences*, *40*(7), 1689–1708.

Cash, B. A., Barimalala, R., Kinter, J. L., Altshuler, E. L., Fennessy, M. J., Manganello, J. V., et al. (2017). Sampling variability and the changing ENSO–monsoon relationship. *Climate Dynamics*, *48*(11-12), 4071–4079.

Compo, G. P., Whitaker, J. S., Sardeshmukh, P. D., Matsui, N., Allan, R. J., Yin, X., et al. (2011). The twentieth century reanalysis project. *Quarterly Journal of the Royal Meteorological Society*, *137*(654), 1–28.

Dawson, A., Matthews, A. J., & Stevens, D. P. (2011). Rossby wave dynamics of the North Pacific extra-tropical response to El Nino: Importance of the basic state in coupled GCMs. *Climate Dynamics*, *37*(1-2), 391–405.

Dee, D. P., Uppala, S., Simmons, A., Berrisford, P., Poli, P., Kobayashi, S., et al. (2011). The ERA-Interim reanalysis: Configuration and performance of the data assimilation system. *Quarterly Journal of the royal meteorological society*, *137*(656), 553–597.

DelSole, T., & Shukla, J. (2012). Climate models produce skillful predictions of Indian summer monsoon rainfall. *Geophysical Research Letters*, *39*, L09703. https://doi.org/10.1029/2012GL051279

Deser, C., Phillips, A. S., & Alexander, M. A. (2010). Twentieth century tropical sea surface temperature trends revisited. *Geophysical Research Letters*, *37*, L10701. https://doi.org/10.1029/2010GL043321

Diaz, H. F., Hoerling, M. P., & Eischeid, J. K. (2001). ENSO variability, teleconnections and climate change. *International Journal of Climatology*, *21*(15), 1845–1862.

Drouard, M., & Woollings, T. (2018). Contrasting mechanisms of summer blocking over western Eurasia. *Geophysical Research Letters*, *45*, 12–040. https://doi.org/10.1029/2018GL079894

Gershunov, A., Schneider, N., & Barnett, T. (2001). Low-frequency modulation of the ENSO–Indian monsoon rainfall relationship: Signal or noise?. *Journal of Climate*, *14*(11), 2486–2492.

Harris, I., Jones, P. D., Osborn, T. J., & Lister, D. H. (2014). Updated high-resolution grids of monthly climatic observations—The CRU TS3. 10 Dataset. *International Journal of Climatology*, *34*(3), 623–642.

Hoskins, B. J., & Karoly, D. J. (1981). The steady linear response of a spherical atmosphere to thermal and orographic forcing. *Journal of the Atmospheric Sciences*, *38*(6), 1179–1196.

Kalnay, E., Kanamitsu, M., Kistler, R., Collins, W., Deaven, D., Gandin, L., et al. (1996). The NCEP/NCAR 40-year reanalysis project. *Bulletin of the American meteorological Society*, *77*(3), 437–472.

L'Heureux, M. L., Lee, S., & Lyon, B. (2013). Recent multidecadal strengthening of the Walker circulation across the tropical Pacific. *Nature Climate Change*, *3*(6), 571.

Minobe, S., & Mantua, N. (1999). Interdecadal modulation of interannual atmospheric and oceanic variability over the North Pacific. *Progress in Oceanography*, *43*(2-4), 163–192.

O'Reilly, C. H. (2018). Interdecadal variability of the ENSO teleconnection to the wintertime North Pacific. *Climate Dynamics*, *51*(9-10), 3333–3350.

O'Reilly, C. H., Heatley, J., MacLeod, D., Weisheimer, A., Palmer, T. N., Schaller, N., & Woollings, T. (2017). Variability in seasonal forecast skill of Northern Hemisphere winters over the twentieth century. *Geophysical Research Letters*, *44*, 5729–5738. https://doi.org/10.1002/2017GL073736

O'Reilly, C. H., Woollings, T., Zanna, L., & Weisheimer, A. (2018). The impact of tropical precipitation on summertime Euro-Atlantic circulation via a circumglobal wave train. *Journal of Climate*, *31*(16), 6481–6504.

Poli, P., Hersbach, H., Dee, D. P., Berrisford, P., Simmons, A. J., Vitart, F., et al. (2016). ERA-20C: An atmospheric reanalysis of the twentieth century. *Journal of Climate*, *29*(11), 4083–4097.

Rayner, N., Parker, D. E., Horton, E., Folland, C., Alexander, L., Rowell, D., et al. (2003). Global analyses of sea surface temperature, sea ice, and night marine air temperature since the late nineteenth century. *Journal of Geophysical Research*, *108*(D14), 4407. https://doi.org/10.1029/2002JD002670

Ropelewski, C. F., & Halpert, M. S. (1987). Global and regional scale precipitation patterns associated with the El Niño/Southern Oscillation. *Monthly Weather Review*, *115*(8), 1606–1626.

Sardeshmukh, P. D., & Hoskins, B. J. (1988). The generation of global rotational flow by steady idealized tropical divergence. *Journal of the Atmospheric Sciences*, *45*(7), 1228–1251.

Schneidereit, A., Schubert, S., Vargin, P., Lunkeit, F., Zhu, X., Peters, D. H., & Fraedrich, K. (2012). Large-scale flow and the long-lasting blocking high over Russia: Summer 2010. *Monthly Weather Review*, *140*(9), 2967–2981.

Shaman, J. (2014a). The seasonal effects of ENSO on European precipitation: Observational analysis. *Journal of Climate*, *27*(17), 6423–6438.

Shaman, J. (2014b). The seasonal effects of ENSO on atmospheric conditions associated with European precipitation: Model simulations of seasonal teleconnections. *Journal of Climate*, *27*(3), 1010–1028.

Shaman, J., & Tziperman, E. (2007). Summertime ENSO–North African–Asian jet teleconnection and implications for the Indian monsoons. *Geophysical Research Letters*, *34*, L11702. https://doi.org/10.1029/2006GL029143

Shaman, J., & Tziperman, E. (2011). An atmospheric teleconnection linking ENSO and southwestern European precipitation. *Journal of Climate*, *24*(1), 124–139.

Trenberth, K. E. (1997). The definition of El Nino. *Bulletin of the American Meteorological Society*, *78*(12), 2771–2778.

Trenberth, K. E., Branstator, G. W., Karoly, D., Kumar, A., Lau, N.-C., & Ropelewski, C. (1998). Progress during TOGA in understanding and modeling global teleconnections associated with tropical sea surface temperatures. *Journal of Geophysical Research*, *103*(C7), 14,291–14,324.

Uppala, S. M., Kållberg, P., Simmons, A., Andrae, U., Bechtold, V. D. C., Fiorino, M., et al. (2005). The ERA-40 re-analysis. *Quarterly Journal of the Royal Meteorological Society*, *131*(612), 2961–3012.

Weisheimer, A., Schaller, N., O'Reilly, C., MacLeod, D. A., & Palmer, T. (2017). Atmospheric seasonal forecasts of the twentieth century: Multi-decadal variability in predictive skill of the winter North Atlantic Oscillation (NAO) and their potential value for extreme event attribution. *Quarterly Journal of the Royal Meteorological Society*, *143*(703), 917–926.

Wulff, COle, Greatbatch, R. J., Domeisen, D. I., Gollan, G., & Hansen, F. (2017). Tropical forcing of the Summer East Atlantic pattern. *Geophysical Research Letters*, *44*, 11,166–11,173. https://doi.org/10.1002/2017GL075493

Yun, K.-S., & Timmermann, A. (2018). Decadal monsoon-ENSO relationships reexamined. *Geophysical Research Letters*, *45*, 2014–2021. https://doi.org/10.1002/2017GL076912